arXiv:1303.2099v3 [cond-mat.str-el] 18 Apr 2013

Effective crystal field and Fermi surface topology: a comparison of d- and dp-orbital models

N. Parragh[1], G. Sangiovanni[1], P. Hansmann[2], S. Hummel[3], K. Held[3], and A. Toschi[3]
[1] *Institut für Theoretische Physik und Astrophysik, University of Würzburg, Germany,*
[2] *Centre de Physique Théorique, Ecole Polytechnique, CNRS UMR7644, 91128 Palaiseau, France*
[3] *Institute of Solid State Physics, Vienna University of Technology, Austria*

The effect of electronic correlations to enhance or reduce the effective crystal field in multi-orbital correlated materials can be crucial in determining the topology of the Fermi surface and, hence, the physical properties of these systems. In this respect, recent local density approximation (LDA) plus dynamical mean-field theory (DMFT) studies of Ni-based heterostructure have shown contradicting results, depending on whether the less correlated p orbitals are included or not. We clarify the origin of this problem and identify the key parameters controlling the Fermi surface properties of these systems. A particularly important one is the filling of the identified d-orbitals: in the dp-calculation this is typically larger so that Hund's exchange leads to a different local magnetic moment for the dp-model.

PACS numbers: 71.10.-w, 71.27.+a, 73.40.-c

I. INTRODUCTION

Correlated electronic systems display some of the most fascinating phenomena in the solid state physics. One of their typical characteristic is a strong sensitivity to small changes of external control parameters. Hence, a precise understanding of the underlying physics and of the pivotal parameters controlling the observed phenomenology represents a crucial goal in contemporary condensed matter research, also in light of possible applications beyond the purely scientific context.

The intrinsic complexity of many-body physics prevents an exact ab-initio theoretical description of correlated materials. In fact, even one of the most basic models for electronic correlations, i.e. the Hubbard model[1] where only the local part of the Coulomb interaction is retained, cannot be exactly solved in the relevant cases of two or three dimensions. However, a great step forward in the theoretical analysis of electronic correlation in condensed matter was achieved in the last decades by means of dynamical mean-field theory (DMFT)[2, 3], and, for realistic material calculations, by its merger with ab-initio density functional approaches (LDA+DMFT)[4].

From the theoretical point of view, DMFT-based methods can be viewed as a quantum extension of the classical mean-field approaches. Hence, the application of DMFT implies neglecting all non-local spatial correlations beyond the standard (static) mean-field theory level. At the same time, DMFT as well as LDA+DMFT, allows for a very accurate (and non-perturbative) treatment of the most relevant part of the electronic correlations stemming from the (single or multi-orbital) Hubbard interaction, i.e. their purely local part. The ability of DMFT to capture these local quantum fluctuations is one of the keys behind its success in addressing many open questions in the physics of strongly correlated materials. Among those, we recall the pioneering DMFT description of the Mott[5] metal-insulator transition (MIT) in V_2O_3[3, 6], of the δ phase of Pu[7], of the correlation effects[8] in Fe and Ni, of the volume collapse in Ce[9], of the unconventional pairing mechanism of superconductivity in fullerenes[10]; most recently DMFT has been also successfully applied to the analysis of the occurrence of kinks in the self-energy[11] and in the specific heat[12] of particular vanadates, such as $SrVO_3$, and LiV_2O_4, as well as of the spectral and magnetic properties[13] of Fe-based superconductors.

Furthermore, it should also be recalled here, that DMFT is a very flexible scheme, whose application is possible also beyond the standard case of bulk correlated systems. In fact, DMFT-based methods have been recently used to study correlated nanoscopic[14] and hetero-structures[15–17]. For the latter case, we want to focus here, in particular, on the theoretical predictions for the Fermi-surface properties of layered Ni-based heterostructures. The application of LDA+DMFT to this problem, and more specifically, to the case of a 1 : 1 layered $LaNiO_3/LaAlO_3$ heterostructure has raised a considerable interest, as the DMFT results of Refs. [17, 18] clearly prospect the possibility to drive the Fermi surface "topology" of these materials very close to the one of the high-temperature superconducting cuprates. In fact, the electronic structure in the bulk Nickelates, such as $R_{1-x}Sr_xNiO_4$, is typically characterized by *two* bands crossing the Fermi level[19], which arise from the two e_g orbitals of Ni (the "planar" x^2-y^2 and "axial" $3z^2-r^2$ orbital). However, by growing heterostructures with planes of $LaNiO_3$ intercalated with insulating planes of $LaAlO_3$ and on substrates providing an epitaxial strain, such as $SrTiO_3$ or $PrScO_3$, the energetic configuration of the $3z^2-r^2$ will be correspondingly disfavored[20], which corresponds to a (positive) crystal field splitting $\Delta_{CF} = \varepsilon_{3z^2-r^2} - \varepsilon_{x^2-y^2} > 0$ among the two e_g-Ni orbitals. In this situation, LDA+DMFT calculations have shown that the inclusion of the correlation effects will always increase the original (LDA) crystal field splitting Δ_{CF} among the two e_g orbitals, leading, eventually, to a significant change of the "topology" of the Fermi surface, i.e. to a situation in which only *one* band, with predominant x^2-y^2 character crosses the Fermi level. Hence, according to these LDA+DMFT calculations, in Ni-based heterostructures it would be possible to "artificially" realize the electronic configuration of the high-temperature superconducting cuprates (i.e., single, almost half-filled orbital with x^2-y^2 symmetry close the Fermi level), e.g. by modulating the strain through changing the substrate or the insulating layer. As the control of the low-Fermi surface properties represents an essential ingredient for novel, alternative, realizations of high-temperature superconductivity, the importance of having highly accurate LDA+DMFT predictions becomes a crucial factor for engineering new materials.

In contrast to these impressive applications of DMFT-based methods, one important aspect should be stressed here: most of the above-mentioned DMFT or LDA+DMFT calculations have been performed by applying DMFT to a "reduced" basis-set including only the most important correlated *d*-orbitals close to the Fermi level.

In the last years, several LDA+DMFT calculations included also the less correlated, typically ligand *p*, orbitals. In most of the cases, these additional (*p*) orbitals were way more extended than the correlated ones (e.g. *d*), and, hence, the local Coulomb interaction between electrons occupying these additional orbitals (U_{pp}) and between electrons on different orbital manifolds (U_{pd}) was either completely neglected, or, at most, treated at the Hartree level[21]. Despite this approximation, it is quite reasonable to expect that the accuracy of LDA+DMFT calculations performed in an enlarged (say: *dp*) basis-set to be higher than the corresponding ones in the restricted *d* manifold. In fact, quite generally: (i) performing a local (Wannier[22], NMTO[23], etc.) projection on an enlarged basis set allows for a better localization of the orbitals of the correlated manifold (as the *dp*-hopping processes are now explicitly included in the model); and (ii) the possibility of describing explicitly charge-transfer processes between the *d* and *p* orbitals makes evidently closer the theoretical modeling to the actual material physics.

Notwithstanding these quite general arguments, when actually performing LDA+DMFT calculations on enlarged *dp* basis-sets the improvement w.r.t. older LDA+DMFT calculations restricted to purely *d*-basis is not always evident. Comparing with experiments, there are cases in which the use of the larger *dp* basis-set makes the accuracy of the theoretical description surprisingly worse. Without attempting to give a complete review here, we recall that LDA+DMFT calculations including *p* orbitals have improved the descriptions of the insulating behavior of NiO[24] and of the MIT in $\mathrm{NiS_2}$[25] w.r.t. *d* only calculations[26]. Also quite accurate results have been obtained for one- and two-particle properties of cobaltates (such as $\mathrm{SrCoO_3}$[27] and $\mathrm{LaCoO_3}$ [28]) and for the well-known class of iron-pnictides and calchogenides[29].

In contrast to the aforementioned successful applications of *dp* calculations, in other, equally important, cases the *dp* LDA+DMFT results are in partial or total contradiction with the *d*-only calculations, and/or with the experimental findings: No MIT in $\mathrm{V_2O_3}$ was found up to very large values of the Coulomb interaction if the oxygen *p* orbitals are included in LDA+DMFT calculations [30]. More recently also the Mott-Hubbard insulating phase of $\mathrm{La_2CuO_4}$ and $\mathrm{LaNiO_3}$ was reported to be missing in the *dp* framework[31], while these materials are found to be insulating in *d*-only calculations for plausible values of the *dd* interaction. These discrepancies between *d*-only and *dp*-calculations regarding the Mott-Hubbard MIT have already raised a discussion in the recent literature. In Ref. [31], non-local correlations neglected by DMFT have been considered as a cause of the discrepancy. In fact, a major role in the determining the onset of insulating cases is likely played also by non-local correlations, especially in the two-dimensional cuprates.

However, there are also other discrepancies, whose discussion will be at the center of this work, which can be hardly attributed to the effects of non local-correlations. These discrepancies are observed for systems of more than one correlated *d* orbital and in broad parameter regimes (including high-T), where effects beyond DMFT should not play any crucial role. In particular, a striking disagreement between *d*-only and *dp*-calculations was reported for the above-mentioned case of Ni-based heterostructures. In fact, LDA+DMFT calculations performed including also the *p*-Oxygen orbitals have shown[32] exactly the opposite trend w.r.t. the previous ones: Even in presence of a favorable crystal field splitting $\Delta_{CF} = \varepsilon_{3z^2-r^2} - \varepsilon_{x^2-y^2} > 0$ at the starting (LDA) level, the net effect of the Hubbard interaction was *always* to reduce the orbital polarization by filling back the $3z^2-r^2$ orbital, which would prohibit "de facto" any possibility of realizing the cuprate conditions for the onset of an unconventional superconductivity.

This second kind of discrepancies between LDA+DMFT performed with different (*d*-only vs. *dp*) basis-sets well illustrated by the contradicting results for the Ni-based heterostructures, raises a quite general question about the proper use and interpretation of the growing number of LDA+DMFT calculations on extended basis sets. The correct determination of the orbital polarization and Fermi surface properties is of great importance for future calculations of increasingly complex materials.

In this paper we aim at understanding the relations between the results of LDA+DMFT calculations on different basis-sets for the Fermi surface properties of multi-orbital systems, and, ultimately, the origin of the qualitative discrepancies, observed by following the standard implementation of the algorithms in different basis-sets. For this purpose, it is of primary importance to disentangle the main, qualitative, trends from the specific features of a selected case. Hence, we will select two (corresponding) minimal models for d-only and dp calculations. They are intended to capture the above-mentioned discrepancy for the prediction of the Fermi surfaces of correlated multi-orbital systems, and allow for a systematic study of this problem.

The scheme of the paper is the following: In Sec. 2 we introduce the simplified models for capturing the discrepancy between the theoretical predictions for the Fermi surface properties of multi-orbital d and dp systems, such as those reported for realistic calculations of Ni-based materials. In Sec. 3, we analyze the effective crystal field splitting and discrepancies between d- and dp-model at for a fixed set of interaction parameters. At the end of Sec. 3, we also provide an analysis of the role of Hund's exchange J. In Sec. 4 we study the origin of the observed discrepancies by analyzing the dependence on the d-electron-density, and we discuss its possible relation with the crossover[33] from high-spin (Hund's regime) to low-spin (CF regime). Finally, in Sec. 5 we summarize our results.

II. MODELS AND METHODS

In this section, we illustrate the simplified minimal model that we have selected to analyze the discrepancies between the LDA+DMFT calculations on different (d-only vs. dp) basis-sets for the prediction of the orbital polarization and the Fermi surface properties of correlated multi-orbital systems. As discussed in the Introduction, we know from preceding d-only and dp studies on bulk Nickelates[19] and Ni-based heterostructures[17, 18], that important discrepancies in the theoretical predictions emerged already when considering the simplest case of two correlated (namely, e_g) orbitals [34]

Hence, here, we set up two models with cubic/tetragonal symmetry to address precisely this issue. The models are obviously inspired by the realistic calculations of nickelate heterostructures, i.e. with a focus on the orbital polarization in a quasi two-dimensional geometry. However, as we are presenting DMFT calculations, the "dimensionality" comes into play only via the k-summations defining the local quantities, and, therefore, the numerical results at the DMFT level will depend mainly on the kinetic energy of the two e_g orbitals, and on its relation w.r.t. the hybridization terms. Hence, the knowledge emerging from our analysis will also be used to clarify the general trends of the multiorbital physics *at the DMFT level.*

Specifically, we will consider two models:

1. The first one is the d-only two-orbital model (Fig.1 upper panels) with the two orbitals representing two e_g orbitals.

2. The second model is a dp four-band model (Fig.1 lower panels) which, in addition to the Nickel $3d - e_g$ states incorporates two oxygen $2p$ states explicitly.

Aiming at understanding the difference in orbital polarization between the two models for a given electronic configuration, we have simplified each model to the minimal set of parameters necessary to describe a physically realistic situation, without too many material specific details. The two models are described below:

d-only two-band model

For the e_g only model in its simplest version we have only two parameters: Hopping amplitude t_{dd} and initial crystal field potential Δ_{CF}. The hopping was parametrized by means of cubic harmonics with the well known table of Slater and Koster [36] while the crystal field potential Δ_{CF} accounts for the on-site energy difference between the two e_g states (i.e. it corresponds to a tetragonal distortion, a compression or elongation along one of the cubic C^4 axes, of the ligand octahedron).

In addition, we pose a restriction to the filling, chosen to be one electron in the two *effective* e_g states, corresponding to the downfolded states which are by no means of pure d-character. In fact, for the nickelates the two bands are the anti-bonding hybrid between the on-site-d and the ligand-p. The effective Hamiltonian in momentum space reads:

$$H^{\mathrm{2b}}_{\mathbf{k}} = \begin{pmatrix} -\frac{3}{2}t_{dd}(\cos k_x + \cos k_y) & -\frac{\sqrt{3}}{2}t_{dd}(\cos k_x - \cos k_y) \\ -\frac{\sqrt{3}}{2}t_{dd}(\cos k_x - \cos k_y) & -\frac{1}{2}t_{dd}(\cos k_x + \cos k_y) + \Delta_{CF} \end{pmatrix}, \tag{1}$$

where the diagonal entries represent the hopping from a x^2-y^2 ($3z^2-r^2$) to a x^2-y^2 ($3z^2-r^2$) in the next unit cell and the off diagonal elements represent the non-local e_g-e_g hybridization (cf. upper inset of Fig.1). Note in case of the heterostructure there is a quasi two-dimensional hopping geometry without hopping along the c-axis. This is why the $3z^2-r^2$ has smaller hopping amplitudes and, consequently, a smaller bandwidth. A related two-band model Hamiltonian, but without hybridization between the orbitals, has been studied in DMFT in Ref. [33], with reference to the cases of BaVS$_3$ and Na$_x$CoO$_2$.

On the upper panels of Fig.1 we show the correspond-

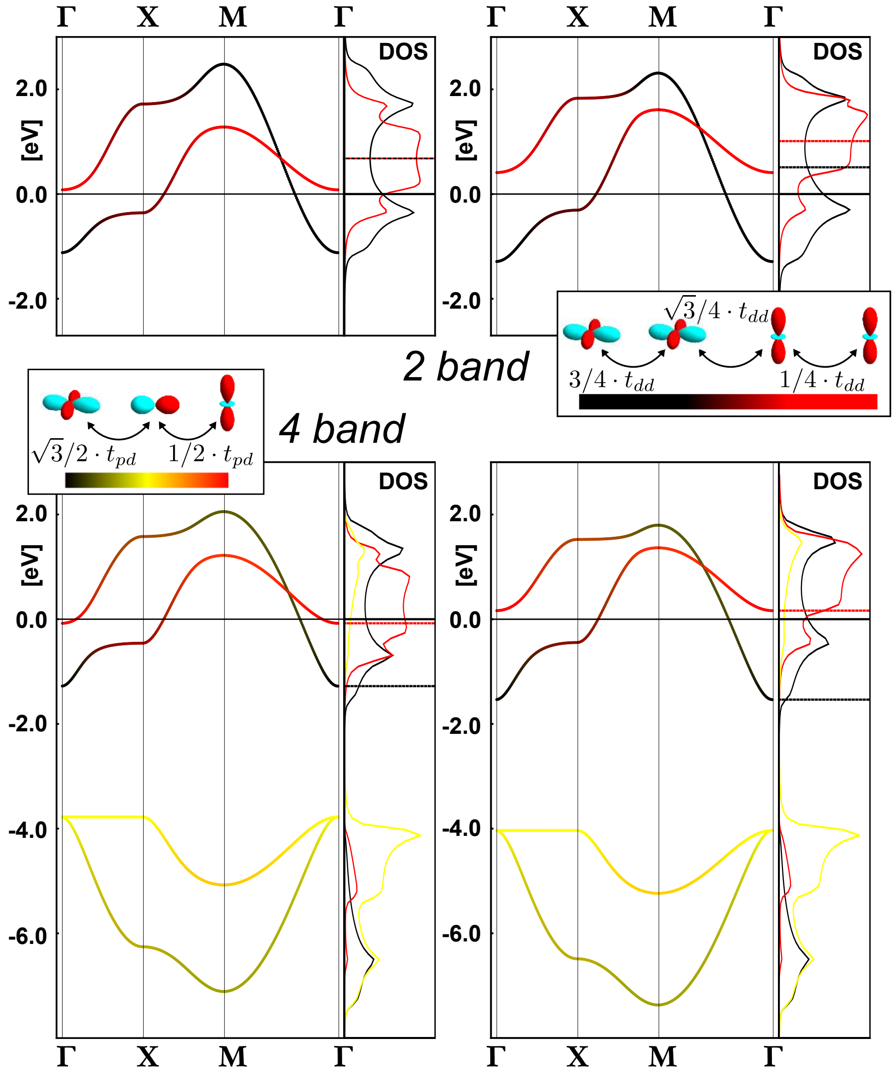

FIG. 1. Band-structure and DOS of the two-band d-model (upper panel) and the four-band dp-model (lower panel) for two different values of the crystal field splitting Δ_{CF} between the two d-orbitals, i.e. $\Delta_{CF} = 0$ (left panels) and 0.5 (right panels). The orbital character is denoted by the following color-coding: black for the first d-orbital ($x^2 - y^2$), red for the second ($3z^2 - r^2$), and yellow for the p-orbitals. In the inset, the hopping processes for the two models are visualized.

ing band structure and single particle density of states (DOS). The color code denotes the orbital character: black and red represent the $x^2 - y^2$- and $3z^2 - r^2$-orbital, respectively. While locally the two orbitals are eigenstates of the tetragonal point group and do not hybridize (pure black/red color of the DOS) the e_g orbitals obviously hybridize non-locally along certain directions (dark-red color, e.g. at the X point of the Brillouin zone). For the model we fixed the hopping amplitude to a value $t_{dd} = 0.6$eV, which leads to a bandwidth comparable to that of NMTO downfolding for the nickelate compounds[17, 18]. The crystal field is the parameter for which we study several cases ranging from -0.5eV to 0.5eV. In the upper panels of Fig. 1 we show two cases $\Delta_{CF} = \{0.0\text{eV}, 0.5\text{eV}\}$ as examples. The value of the local splitting can also be found in the difference of the center of mass of the DOS (drawn as dashed black/red lines).

dp four-band model

The second model we treat is in a way the "upfolded" version of the two-band model just described. We added two oxygen ligand orbitals in the quasi two dimensional geometry of the model which can be thought of as one p_x and one p_y orbital on each oxygen site. This is the minimal dp-model that can be constructed with a realistic dp-configuration in a quasi two dimensional cubic/tetragonal symmetry. For this upfolded model additional parameters have to be assigned and chosen to be in correspondence with the two-band model: the parameters (hopping amplitude and orbital splitting) of the d-only model should, as effective parameters, be derivable from the parameters of the four-band model. Specifically, for the orbital splitting we remark that the formerly labeled "crystal field" splitting is, in fact, a "ligand field" splitting which can be in principle decomposed into an electrostatic Madelung potential and a *dp*-hybridization splitting. Moreover, the dd-hopping processes are, in fact mediated by oxygen *p*-orbitals and we do not have a direct *dd*-hopping in the four-band model. Keeping this in mind, we choose the parameters (*dp*-hopping amplitude and on-site d/p energies) in a way that the two bands at the Fermi energy (which are the anti-bonding *dp*-hybrid) reproduce the two bands of the previous model. We stress already at this point, however, that our subsequent results are robust with respect to the details of these parameters. The *dp*-Hamiltonian in momentum space reads:

$$H^{\rm 4b}_{\mathbf{k}} = \begin{pmatrix} 0 & 0 & i\sqrt{3}t_{pd}\sin\left(\frac{k_x}{2}\right) & -i\sqrt{3}t_{pd}\sin\left(\frac{k_y}{2}\right) \\ 0 & 2t_{dd}+\Delta_{CF} & it_{pd}\sin\left(\frac{k_x}{2}\right) & it_{pd}\sin\left(\frac{k_y}{2}\right) \\ -i\sqrt{3}t_{pd}\sin\left(\frac{k_x}{2}\right) & -it_{pd}\sin\left(\frac{k_x}{2}\right) & \epsilon_p & 0 \\ i\sqrt{3}t_{pd}\sin\left(\frac{k_y}{2}\right) & -it_{pd}\sin\left(\frac{k_y}{2}\right) & 0 & \epsilon_p \end{pmatrix}, \tag{2}$$

where t_{dd} and Δ_{CF} are the parameters of the corresponding two-band model and $t_{pd} = 3 \cdot t_{dd}$ was chosen to yield the same bandwidth for the antibonding bands as in the previous model. The energy of the *p*-states was fixed to $\epsilon_p = -2.5$eV similar to the position of the p-bands in the nickelate systems.

In the lower panels of Fig. 1 we show the bandstructure of the four-band *dp*-model for the same crystal field splitting as for the two-band model. In the bandstructure and DOS plots the additional yellow color encodes the p-character.

DMFT for dp-models with projections

Extended models including ligand *p*-states explicitly have a structure like our 4-band Hamiltonian (2). Locally, i.e. integrated over the Brillouin zone, such Hamiltonians have the form:

$$H^{\rm loc.}_{\rm full}(R=0) = \begin{pmatrix} H^{\rm loc.}_{dd} & H^{\rm hyb.}_{dp} \\ \left(H^{\rm hyb.}_{dp}\right)^{\dagger} & H^{\rm loc.}_{pp} \end{pmatrix} \tag{3}$$

The local basis is typically chosen in a way that the H_{dd} and H_{pp} blocks are diagonal after $\mathbf{k}$–integration so that the states can be labeled by a good *local* quantum number in the respective subspaces, such as the crystal field labels (see DOS plots in Fig. 1). In such a basis, the local Coulomb (U) matrix of the interacting part of the Hamiltonian is then defined (in its SU(2)-invariant "Kanamori") form as

$$\begin{aligned} H_{loc} = \; & \textstyle\sum_a U n_{a,\uparrow} n_{a,\downarrow} \\ & + \textstyle\sum_{a>b,\sigma} \left[U' n_{a,\sigma} n_{b,-\sigma} + (U'-J) n_{a,\sigma} n_{b,\sigma}\right] \\ & - \textstyle\sum_{a\neq b} J (d^{\dagger}_{a,\downarrow} d^{\dagger}_{b,\uparrow} d_{b,\downarrow} d_{a,\uparrow} + d^{\dagger}_{b,\uparrow} d^{\dagger}_{b,\downarrow} d_{a,\uparrow} d_{a,\downarrow} + h.c.). \end{aligned}$$

for the *d*-orbital sector. Here, U denotes the interaction parameter between two electrons in the same *d*-orbital, U' the interaction between electrons on different *d*-orbitals and J is the Hund's coupling; a, b index the two orbitals and σ the spin. Note that the specific interaction values for the DMFT calculations (see next section for details) have been chosen in order to reproduce a typical correlated metallic physics situation. Obviously, due to the stronger localization of the *d*-orbitals in the *dp* models, the corresponding values of the local interaction on the *d* orbitals have been correspondingly enhanced (we assumed here a factor two for the parameter U'). We recall that –for the *dp* case– the multi–orbital Hubbard interaction could include, besides on-site *d*– and on-site *p*–interactions, also possible *dp*–interactions. This is, however, not the topic of the present study. Further, for the *dp* model in LDA+DMFT we have to face the so-called problem of *double counting correction* (DC)[4, 37, 38]: This does no longer correspond to a simple total energy shift and, hence, cannot be "absorbed" in the chemical potential. The DC for the *dp*-models corresponds to a renormalization of the energy difference between d and p states. For our models we have used the DC suggested by Anisimov [37], given by:

$$\begin{aligned} \bar{U}_{dd} &= \left[U + U'(N_d-1) + (U'-J)(N_d-1)\right]/\left(2N_d-1\right) \\ \Delta_{DC} &= \bar{U}_{dd}(\textstyle\sum_d n_d^{LDA} - 0.5), \end{aligned} \tag{4}$$

where N_d is the number of $d-$orbitals, and $\bar{U}_{dd}$ is the average local interaction between these d-orbitals; n_d^{LDA} denotes the occupation of the $d-$orbitals as calculated from the **k**-resolved non-interacting (LDA) Hamiltonian discussed above.

The self-consistent DMFT loop, which includes the solution of an Anderson impurity problem for the correlated subspace at each step is done as follows:

1. The first step is the calculation of the **k**–integrated Green function on the *full dp* basis set:

$$G_{\text{full}}^{\text{loc.}}(\omega) = \frac{1}{V_{\text{BZ}}} \int_{\text{BZ}} d^3k \left[(\omega+\mu)\mathbf{1} - H(\mathbf{k}) - \Sigma_{\text{full}}(\omega)\right]^{-1} \tag{5}$$

   where G, Σ, and H are matrices on the *dp*-basis.

2. Next, we extract the *dd*-block of the local Green function:

$$G_{dd}^{\text{loc.}}(\omega) = \left\{G_{\text{full}}^{\text{loc.}}(\omega)\right\}|_{dd-\text{block}}, \tag{6}$$

   i.e. we project it onto the *d*-subspace. We stress here, that due to the *dp* hybridization encoded in the Hamiltonian $H(\mathbf{k})$ and the inversion of Eq. 5 the information about the p–ligands is not lost but captured by $G_d^{\text{loc.}}(\omega)$.

3. Now, in complete analogy to DMFT for *d*–states only, we calculate the Weiss field for the impurity model (only on the d–subspace):

$$\left[\mathcal{G}^0(\omega)\right]^{-1} = \left[G_{dd}(\omega)\right]^{-1} + \Sigma_{dd}^{\text{DMFT}}(\omega), \tag{7}$$

   where $\Sigma_{dd}^{\text{DMFT}}(\omega)$ denotes the DMFT *dd* self-energy.

4. With $\mathcal{G}^0(\omega)$ we solve the auxiliary impurity problem (see below), obtain a new $G_{dd}^{\text{loc.}}$ and with the inverse of Eq. (7) a new $\Sigma_{dd}^{\text{DMFT}}(\omega)$.
   Finally the self-consistent loop is closed by comparing both the new and the old $\Sigma_d^{\text{DMFT}}(\omega)$ *and* the new and the old d/dp-density and iterating until convergence.

As impurity solver for our DMFT calculations, we have used the continuous time quantum Monte-Carlo (QMC) algorithm in the hybridization expansion (CT-HYB)[39, 40], which allows also for the treatment of the spin-flip and pair-hopping terms of our Kanamori Hamiltonian (Eq. 4). In the CT-HYB the time evolution is calculated using the local interaction, which makes the local Hilbert space growing exponentially with the number of orbitals. While for density-density interactions this problem can be mitigated along the line of [39, 41], for the more realistic Kanamori interaction a set of quantum numbers, called PS, leads to a more efficient algorithm [42]. We have used this to perform all calculations presented in this paper with the full SU(2)-symmetric Hamiltonian.

III. RESULTS: *d VS dp* CALCULATIONS AT "QUARTER FILLING"

In this section, we compare our DMFT results for the *d*-only model at quarter-filling ($n_d = 1$) with that of the corresponding *dp* model including also two $2p$ oxygen orbitals below the Fermi level (with a total density $n_{tot} = n_d + n_p = 5$). Specifically, in the next two subsections, we discuss how the final orbital polarization of the *d*-only (Sec. III A) and *dp* calculations (Sec. III B) evolves when varying the values of the initial crystal field splitting Δ_{CF} between the *d*–orbitals. While the model cases studied here do not aim at a realistic description of a specific system, the results of this section can be qualitatively related, depending on the value of $\Delta_{CF} = \varepsilon_{3z^2-r^2} - \varepsilon_{x^2-y^2}$, to the physics of bulk Nickelates[19] and of Ni-bases heterostructures[17, 18, 32]. In fact, (i) the nominal charge of these systems corresponds also to one electron in the outer two Ni-bands and (ii) the bulk Nickelates are typically characterized by negative values of Δ_{CF}, because of the tetragonal distortion along the z axis. In the Ni-based heterostructures instead, the localization effects in the z direction, as well as the epitaxial strain due to the substrate, induce positive values for Δ_{CF}.

A. DMFT results for the *d*-only model

In this subsection, we analyze the results for our *d*-only two-orbital model at quarter filling ($n_d = 1$), as a function of the initial crystal field splitting Δ_{CF}: the corresponding results for the orbital occupation without interaction (which carry the label LDA, as this would correspond to the LDA in a realistic calculation) and with the interaction (computed with DMFT) are shown in Fig. 2. As mentioned in Sec. II, the interaction values have been chosen in consideration of typical values for transition metal oxides systems: for the *d* only model, we adopted a value of $U' = U - 2J = 4$ eV, with $J = 0.5$eV.

We start by briefly commenting the set of non-interacting ("LDA") data shown in Fig. 2: They display a monotonous dependence on the initial crystal field: the

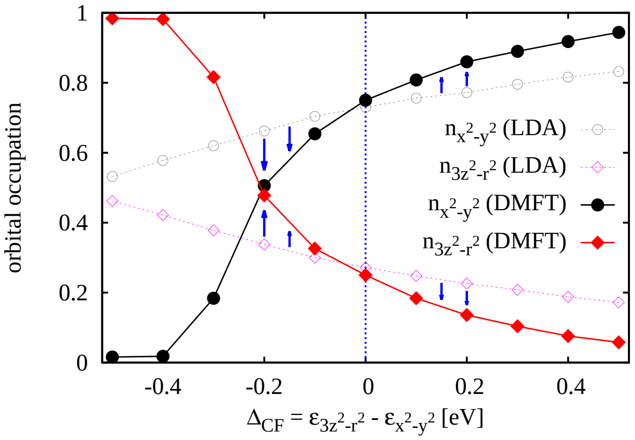

FIG. 2. Orbital occupation of the d-only model with $U' = 4$eV, $J = 0.5$eV ($U = 5$eV), $\beta = 100\text{eV}^{-1}$ at quarter filling ($n_d = 1$) as a function of the initial crystal field splitting Δ_{CF}. The DMFT data (solid symbols) are compared with the corresponding non-interacting results (empty symbols; coined LDA). The arrows indicate the effect of the interaction which is opposite for $\Delta_{CF} > 0 (< 0)$.

orbital occupation of the $x^2 - y^2$ monotonously increases upon increasing values of Δ_{CF}, whereas the occupation of the $3z^2 - r^2$ orbital decreases. We note, however, that as the hopping terms (and, hence, also the bandwidth) for the two orbital are not equal – a quite general situation for realistic material calculations – the orbital occupation curves are not symmetric w.r.t. to Δ_{CF}. This also implies that the situation where the two orbitals are equally occupied (i.e. no orbital polarization) does not occur at $\Delta_{CF} = 0$ but for the non-interacting case only for $\Delta_{CF} < -0.5$eV.

We discuss now the effects of the Hubbard interaction on the orbital occupations, as described by our DMFT(CT-QMC) calculations. While the occupation curves remain obviously asymmetric also in presence of the interactions, from the data of Fig. 2 we note that, for each orbital, the *deviations* w.r.t. to the non-interacting values are strongly dependent on Δ_{CF}. In fact, for all data considered, we observe that the sign of the change in the orbital occupation w.r.t. its LDA value appears closely connected with the sign of Δ_{CF}: For $\Delta_{CF} > 0$ we observe generally an enhancement(reduction) of the occupation of the first(second), $x^2 - y^2$ ($3z^2 - r^2$) orbital, while for $\Delta_{CF} < 0$ the trend is the opposite.

This represents, hence, a very robust behavior for the changes induced by the interaction to the orbital polarization P, which can be formally defined analogously to Refs. [32, 43]

$$P = \frac{n_{x^2-y^2} - n_{3z^2-r^2}}{n_{x^2-y^2} + n_{3z^2-r^2}}. \tag{8}$$

In fact, such a trend explains, on more general grounds, the physics underlying the qualitatively different LDA+DMFT results previously obtained for the shape of the Fermi surface via specific d-only calculations for bulk nickelates[19] and Ni-based heterostructures[17, 18], respectively: The difference in the results simply reflects the different sign of the initial crystal field splitting (Δ_{CF}), as estimated by the ab-initio calculations, whose final size (Δ_{eff}) is always significantly magnified by the electronic interaction.

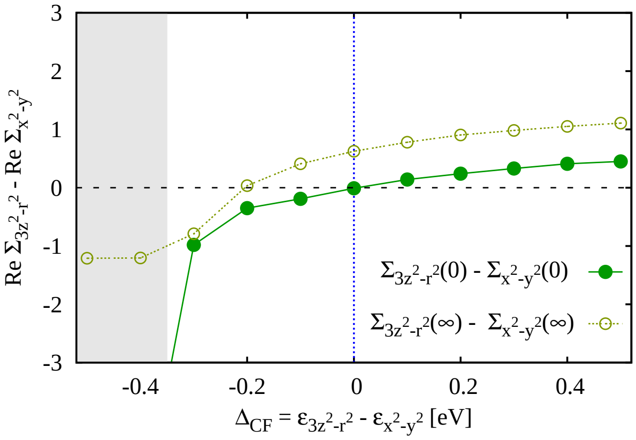

FIG. 3. Difference of the real part of the DMFT self-energies for the two orbitals of the d-only model with $U' = 4$eV, $J = 0.5$eV ($U = 5$eV), $\beta = 100\text{eV}^{-1}$ at quarter filling ($n_d = 1$) extrapolated to $\omega_n \to 0$ (solid symbols) and $\omega_n \to +\infty$ (empty symbol, Hartree contribution to the self-energy) as a function of the initial crystal field splitting Δ_{CF}. The huge enhancement of the difference between the self-energy at $\omega_n \to 0$, and the consequent huge energy shift of the first orbital, marks the onset of the Mott insulating phase (shaded region on the left).

The last statement can be formalized more quantitatively through the analysis of the corresponding self-energies presented in Fig. 3: here we show the differences between the real parts of the DMFT self-energy of the two orbitals, i.e. $\text{Re}\Sigma_{3z^2-r^2}(i\omega_n) - \text{Re}\Sigma_{x^2-y^2}(i\omega_n)$, evaluated in the limit frequency $\omega_n \to 0$ and $\omega_n \to +\infty$, respectively. We recall that in the latter limit only the Hartree contributions to the electronic self-energy remains. Hence, the difference between the self-energies can be also explicitly written in terms of the electronic density as:

$$\begin{aligned} \text{Re}\Sigma_{3z^2-r^2}(\infty) - \text{Re}\Sigma_{x^2-y^2}(\infty) &= (U - 5J) \\ (n_{x^2-y^2} - n_{3z^2-r^2}) &= (U - 5J)\, P. \end{aligned} \tag{9}$$

Here, the last equality only holds at quarter filling where $n_{x^2-y^2} + n_{3z^2-r^2} = 1$. Such a dependence on the (final) electronic density appears evidently in the corresponding data of Fig. 3, where the sign change [44] contribution to the DMFT self-energy is found precisely when the orbital occupations become equal, i.e. for the negative values of $\Delta_{CF} \sim -0.2$ eV for which $P = 0$ in Fig. 2. By comparing this to the previous results and discussions, it should be clear that the high-frequency values of the self-energy do not represent the "crucial" parameter. Instead, the trends in the orbital polarization and, therefore, the predicted physics is controlled by the low-frequency behavior of the self-energy: Up to the point to which the systems still behaves as a (correlated) metal, i.e. when a Fermi surface still exists, the "effective" crystal field determines the splitting between the two orbitals in the presence of electronic correlations. It is given by

$$\Delta_{eff} = \Delta_{CF} + \mathrm{Re}\Sigma_{3z^2-r^2}(0) - \mathrm{Re}\Sigma_{x^2-y^2}(0), \qquad (10)$$

i.e. the original crystal field is corrected by the difference of the real self-energies for $\omega_n \to 0$. This makes evident the interpretation of the second set of data shown in Fig. 3: the sign of $\mathrm{Re}\Sigma_{3z^2-r^2}(0) - \mathrm{Re}\Sigma_{x^2-y^2}(0)$ exactly follows that of the original crystal field Δ_{CF}, and confirms, from the microscopic point of view, the quite robust picture of interaction effects *always* magnifying the size of the original crystal field. Of course the magnification effects will quantitatively depend on many factors. Quite naturally, they will be stronger when the system is more correlated. A dramatic enhancement is found when the Mott metal insulator transition is approached, i.e. when Δ_{CF} approaches the shaded area in Fig. 3. Here the low energy physics correspond to an empty (broader) $x^2 - y^2$ orbital and a half-filled (narrower) $3z^2 - r^2$ orbital.

The coherent picture emerging from these LDA+DMFT, which would also provide a general and solid framework for understanding the previous d-only calculations for bulk nickelates and heterostructures, appears however to be contradicted when extending the basis-set of the LDA+DMFT algorithm to include also the most relevant p degrees of freedom, as it will be shown explicitly in the next subsection.

B. DMFT results for the (corresponding) dp model

We repeat in this subsection the same analysis done above for the d-only model, but now for the calculations performed in the enlarged dp basis set, to study the differences between the two cases. Specifically, we consider here the second model in Sec. 2, including additionally, to the two $d(e_g)$ orbitals, also two p orbitals lying well below the Fermi level. The total occupations is $n_{tot} = n_p + n_d = 5$. Because of the stronger localization of the d–orbitals in the dp case, larger values for U, U' and J have been considered: For the sake of generality [45] , we have simply doubled the value of U' and J w.r.t. the calculation discussed in the previous section, i.e. $U' = 8$eV, $J = 1$eV ($U = U' - 2J$) which correspond, anyhow, to plausible values for correlated orbitals in transition metal oxides.

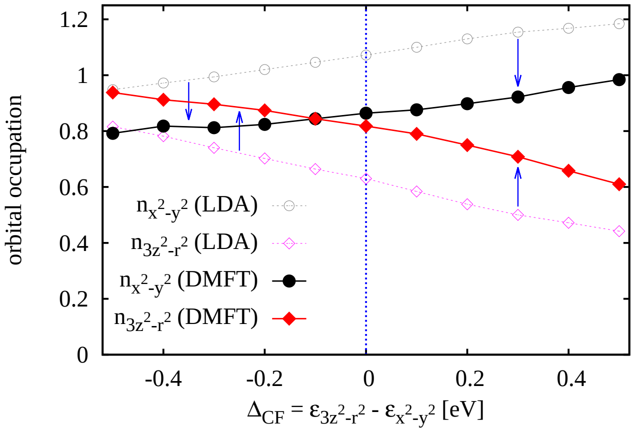

FIG. 4. Orbital occupation of the d orbitals as a function of the initial crystal field splitting Δ_{CF} for the four-band dp model with $U' = 8$eV, $J = 1.0$eV ($U = 10$eV), $\beta = 100\mathrm{eV}^{-1}$ and the filling is $n_{tot} = 5$. The DMFT data (solid symbols) are compared with the corresponding non-interacting results (empty symbols).

As in the previous subsection, we consider first the plot (Fig. 4) of the occupation of the two d-orbitals as a function of the initial crystal field splitting Δ_{CF}, starting from the non-interacting case. While the qualitative behavior as a function of Δ_{CF} appears similar as before, an important difference should be noted: In spite of the relatively large separation (~ 2eV) among d and p band, due to the hybridization between the d and the p manifolds, the total occupation of the d orbitals is now much larger than before ($n_d \sim 1.7 \div 1.8$). Quite remarkably, according to our DMFT results of Fig. 4, such an enhanced occupation of the "correlated" d orbitals survives basically unchanged also when switching on the local interaction.

This fact has an obvious impact on the final results for the orbital polarization P, as now the sign of its change w.r.t. the non-interacting case are no longer related to Δ_{CF}: Fig. 4 shows that independently on the sign Δ_{CF}, one *always* observes a reduction of the value of P, i.e. a net enhancement (reduction) of the occupation of the $3z^2 - r^2$ ($x^2 - y^2$) orbital driven by the electronic interaction.

This is evidently confirmed by the analysis of the corresponding self-energies: As discussed before, the most important piece of information here is enclosed in the zero-frequency extrapolation of the real part of the DMFT self-energies. Fig. 5 shows the plot corresponding to Fig. 3 but now for the four-band dp-model: here the interaction correction always reduces the initial crystal field, in agreement with the systematic depletion of the $x^2 - y^2$ orbital (reduction of P) observed in the whole parameter range considered.

The results are therefore in *qualitative* disagreement with those obtained within the d-only model, at least in the region of positive values of the initial crystal field Δ_{CF}. It is worth noticing that for positive values of Δ_{CF}, this trend is consistent with the results of the dp calculations for the Ni-based heterostructures of Ref. [32]: There, it was shown, that even when starting from a

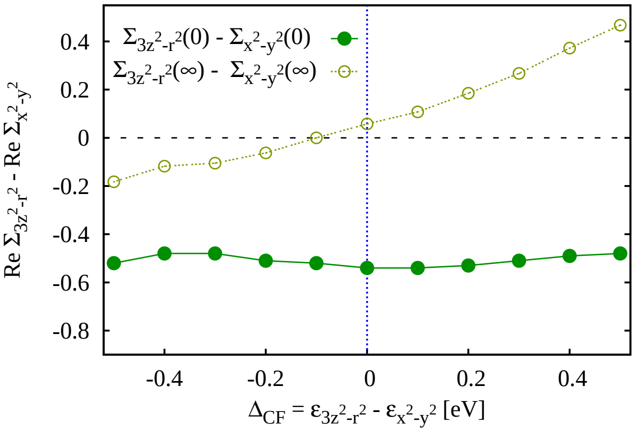

FIG. 5. Difference of the real part of the DMFT self-energies for the two d-orbitals of the four-band dp model as a function of the initial crystal field splitting Δ_{CF} with $U' = 8$eV, $J = 1$eV ($U = 10$eV), $\beta = 100\text{eV}^{-1}$ and the filling is $n_{tot} = 5$. Shown is the low and high frequency asymptotes, i.e. the extrapolation to $\omega_n \to 0$ (solid symbols) and $\omega_n \to +\infty$ (empty symbol, Hartree contribution to the self-energy).

relatively significant orbital polarization for the $x^2 - y^2$ orbital at the LDA level, the polarization was always strongly reduced by the interaction, which obviously has bad implications on the possibility of actually manipulating the Fermi surfaces of the Ni-based heterostructures in the “desired” cuprate-like way [17, 20].

As a matter of fact, this discrepancy between d-only and dp results has now been found here by including the SU(2) symmetry of the local interaction on the e_g bands in both DMFT calculations. This confirms the hypothesis of Ref. [32] that such a discrepancy in the theoretical predictions does not originate from some different treatment of the interactions between the calculations of Refs. [17, 18] and [32], but rather from some intrinsic difference in the calculations. The most evident systematic difference is the filling n_d of the two e_g-orbitals, which, due to the dp hybridization is strongly increased w.r.t. the quarter filling level of the d-only model. While this is rather obvious at the LDA level, we note that the occupation of the d-manifold does not change much even in presence of the interaction, for typical choices of the double-counting term for the DMFT (see Sec. 2, for details, and also Ref. [32]). Quite interestingly, the possible role of an enhanced $d-$orbitals occupations in dp calculations has been also recently addressed, for the different problem of the occurrence of the MIT[31]. Here, besides the role of n_d, or more precisely, connected with it, we note that the final outcome of the results, and, in particular, the occurrence of qualitative discrepancy between d-only and dp-results, is strongly influenced by the value of the Hund's exchange J constant. From the numerical point of view, this is exemplified by the results presented in Fig. 6, where the dp calculations have been performed reducing the value of J from 1.0eV to $J = 0.5$eV, and $J = 0.0$eV ($U' = U - 2J = 8$eV is kept fixed, instead).

The combined analysis of the orbital occupation and of the self-energy (at $\omega_n \to 0$) results shows that the dp results of Fig 4 and 5 change qualitatively already for the case $J = 0.5$eV: the overall trend of strong reduction of occupation of the first $x^2 - y^2$ orbital disappears for a large region of values of the initial crystal field Δ_{CF}. In fact, the results already at J=0.5eV would lead to a physical situation which is qualitatively similar to that predicted by the d-only model. As one can expect, the change with respect to the previous dp results becomes even larger when setting $J = 0.0$eV, as both trends of orbital occupation and effective crystal field becomes exactly opposite, with the orbital $x^2 - y^2$ occupation always increased by the interaction irrespectively of the value of the initial Δ_{CF}. The sensitivity of the final dp results on the Hund's coupling is very illustrative and shows the crucial role of the Hund's exchange in this situations [46].

IV. RESULTS: THE ROLE OF THE d-ORBITAL OCCUPATION

From the marked discrepancy between dp and d calculations, discussed in the previous sections, a general question naturally arises: Under which conditions can one expect to obtain qualitatively similar DMFT results for d-only and dp-calculations? Let us assume here that we have a most accurate estimate [50] of the local interactions and especially the Hund's exchange J. One of the most basic differences between the d-only and the dp calculations examined is the different value of the occupation of the d orbitals. This difference is observed already at the level of the non-interacting “LDA” model and is, remarkably, not strongly affected by the inclusion of the interaction: For the d-only model, the LDA+DMFT calculations have been performed, as usual, at fixed filling, while the value of d-orbital occupation for the dp calculations presents rather moderate oscillations around a much larger value of $n_d \sim 1.75$, quite independently of the parameter set (U,J,Δ_{CF}) considered. Since the filling of the correlated orbitals is a crucial factor to drive the systems towards a Mott-Hubbard MIT, it is logical to suppose that it is also one of the pivotal parameters to be considered when comparing LDA+DMFT calculations on different basis-sets.

To make our statement more quantitative, we have performed several additional DMFT calculations for the same d-only model as in Sec. 2, but now varying systematically n_d from the original quarter-filling level up to the much higher $n_d \sim 1.75$ found in the dp calculations. The results for the orbital occupations and the self-energy at the Fermi level are reported in Fig. 7 in the upper and lower-row panels, respectively. By gradually increasing the total occupation of the d-orbitals, and focusing on the most interesting regime of $\Delta_{CF} > 0$, one observes that the parameter region where the crystal

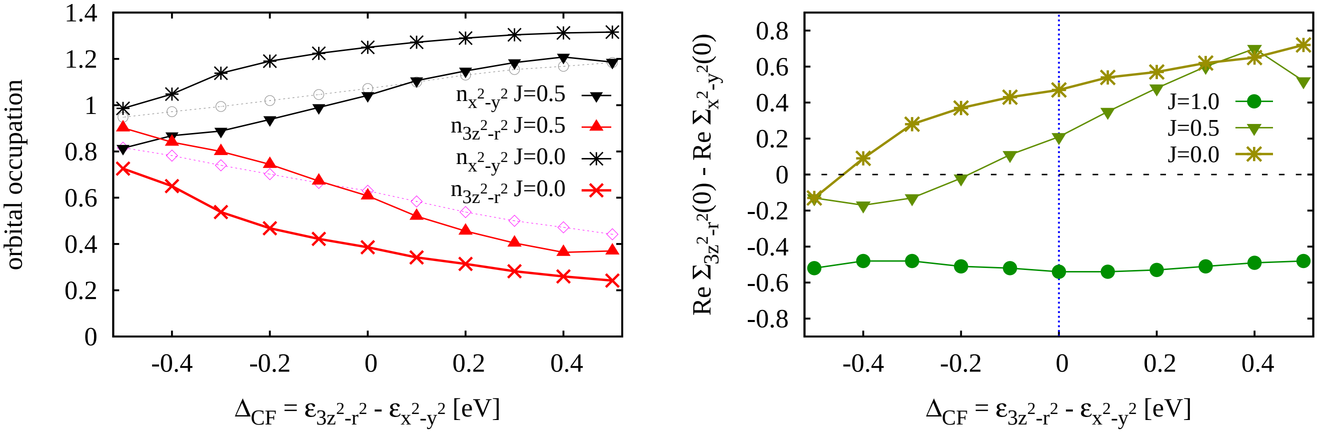

FIG. 6. Left panel: Orbital occupation of the d orbitals of the four-band dp model as a function of the initial crystal field splitting Δ_{CF}. We used $U' = 8$eV, $\beta = 100\text{eV}^{-1}$, $n_{tot} = 5$ and two different values of the Hund's exchange $J = 0.0, 0.5$ eV. The DMFT data (solid symbols) are compared with the corresponding non-interacting results (empty symbols). Right panel: Corresponding data for the difference of the real part of the DMFT self-energies for the two d-orbitals of the four-band dp model extrapolated to $\omega_n \to 0$ as a function of the initial crystal field splitting Δ_{CF}. The self-energy data are also compared with the corresponding DMFT data at $J = 1.0$, previously shown in Fig. 5.

field "drives" the final result (i.e. where its magnitude is enhanced by the interaction), shrinks, being confined to higher and higher values of the initial Δ_{CF}: Looking at the self-energy plot for $n_d = 1.1$, a qualitative change in the trend of the effective crystal field w.r.t. the non-interacting one is found for $\Delta^*_{CF} \sim 0.1$. For $\Delta_{CF} < \Delta^*_{CF}$ the trend for the effective crystal field is *opposite* to that observed for quarter filling, i.e. the original crystal field Δ_{CF} is *reduced* by the interaction. A similar situation, though for a slightly larger threshold ($\Delta^*_{CF} \sim 0.15$), is also observed for the changes in the orbital occupations, w.r.t. the non-interacting ones. By further increasing n_d to 1.25 (second panels of Fig. 7)), the threshold Δ^*_{CF} is already shifted at the border of the parameter region considered ($\Delta^*_{CF} \sim 0.5$). Finally, if one performs the DMFT d-only calculations for a similar $n_d = 1.75$ as in dp-model, one indeed finds similar results as for the dp-model: Both, the effective crystal field and the changes in the relative orbital occupations in Fig. 7, $n_d = 1.75$ resembles those of the dp-model in Figs. 4 and 5.

Let us stress that due to the different bandwidths of the two e_g orbitals, no symmetric behavior between the regions of positive and negative Δ_{CF} can be expected. In fact, in the region $\Delta_{CF} < 0$ (i.e. the less relevant one in the perspective of the Ni-based heterostructures), the crystal field "enhancement" at quarter filling was much larger than the corresponding one for $\Delta_{CF} > 0$ (see Fig. 3), also as an effect of the closer proximity of the MIT in this parameter region. Hence, while the effects of an increased n_d are always at work, here they are just visible as a mere weakening of the quarter fillings trends rather than as of an inversion of them: The gray shadow area, marking the onset of the MIT for one of the two orbitals i.e., the (almost) half-filled one, is shrinking in the $n_d =$ 1.1 plot, and essentially disappears at $n_d = 1.25$. At higher densities, one also observes that the large size of the (negative) effective crystal field for $\Delta_{CF} = -0.5$ is visibly reduced w.r.t. the case of quarter filling.

These results demonstrate the important role played by the density of the d–orbital manifold for determining the final DMFT results on different basis sets, at least for the important aspect of the Fermi surface properties. The starting value of n_d will decide, whether, *given a correct ab-initio estimate* of the interaction parameters of the multi-orbital Hubbard Hamiltonian, the physics of the interacting system will be *driven* by the (original) crystal field, or rather by the Hund's rule tendency for equally occupied orbitals. Therefore, it will be *a priori* quite hard to reconcile DMFT calculations performed on different basis-sets, without considering the corresponding occupation of the correlated orbitals manifolds.

From the perspective of actual material calculations, the strong dependence of the final LDA+DMFT results for the Ni-based heterostructures is now much easier to understand. In fact, the quarter-filling physics particularly favors the crystal field-dominated physics, since the Hund's exchange is weaker in a system with one electron (on average). Hence, if the dp hybridization can drive the system away from this regime (as is the dp model considered here with an average filling of $n_d \sim 1.75$), the Hund's exchange will eventually prevail over the crystal field effects. The same interpretation can likely explain, why the results of LDA+DMFT calculations for the Fe-based superconductors do not display such crucial dependence on the basis-set considered. There, the five orbitals of the Fe-3d manifold are characterized by a very small value of $\Delta_{CF} \sim 0.2$eV (in comparison to the typical values of 1eV observed in many transition

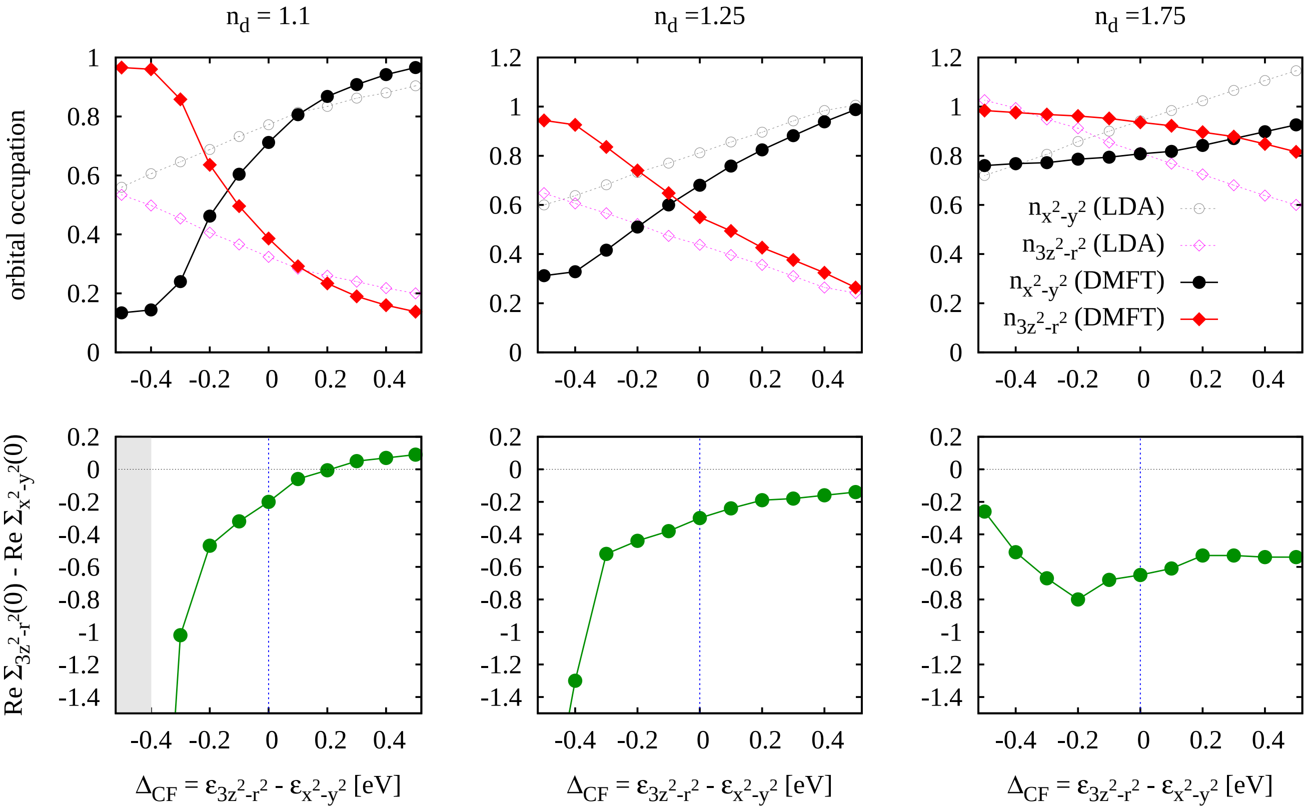

FIG. 7. Upper row: Orbital occupations of the two orbitals of the d-only model with $U' = 4$eV, $J = 0.5$eV ($U = 5$eV), $\beta = 100\text{eV}^{-1}$ for different filling $n_d = 1.1, 1.25, 1.75$ as a function of the initial crystal field splitting Δ_{CF}. The DMFT data (solid symbols) are compared with the corresponding non-interacting results (empty symbols). Note that a filling of $n_d = 1.75$ roughly corresponds to the filling of the two d-orbitals in the dp models considered in the previous sections. Lower row: Difference of the real part of the DMFT self-energies for the two orbitals extrapolated at $\omega_n \to 0$ (solid symbols) as a function of the initial crystal field splitting Δ_{CF} for the corresponding set of data.

metal oxides). This corresponds to a situation of five partially filled ($n_d \sim 6$) correlated orbitals all very close energetically at the Fermi level, i.e. the most favorable playground for strong Hund's exchange processes. Hence, this case is well inside in one of the two regimes, and possible moderate differences in the initial orbital occupation in the d-manifold in different basis-set will *not* result in a qualitative discrepancy between different LDA+DMFT calculations.

V. CONCLUSIONS

We have thoroughly compared two models for transition metal oxides: a d-only model with two effective d-orbitals and a dp-model with two d- and two p-orbitals. On the single-particle level without Coulomb interaction, the two models show the same low-energy physics and band-structure. However if the Coulomb interaction is taken into account by means of LDA+DMFT, this is not the case any more.

The main reason for this discrepancy is the number of d-electrons. In the d-only model there is on average one d-electron per site. For the dp-model on the other hand, the bands are filled with altogether 5 electrons per site: Without hybridization the two p-orbitals at lower energy would be completely filled, and the d-orbitals in the vicinity of the Fermi level would have the same filling (one electron per site) as for the d-only model. The d-orbitals hybridize however with the p-orbitals, and, hence, there is some admixture between the orbitals leading altogether to a larger filling ($\sim$ 1.7) of the d-orbitals for the dp-model.

This different filling has dramatic consequence for the correlated solution of the two models. For the d-only model the Coulomb interaction enhances the initial crystal field splitting, leading to a situation with one d-electron in the lowest-lying d-orbital. Depending on the original crystal field (e.g., if $\Delta_{CF} > 0$), this can be the $x^2 - y^2$-orbital, which hence dominates the low energy physics and Fermi surface topology. This kind of physics can result in a very similar occupation of the $x^2 - y^2$-orbital and Fermi surface in Ni-based heterostructures as in cuprates.

In contrast, for the *dp*-model the Hund's exchange favors a situation with a more even occupation of the two orbitals, an enhancement of the local magnetic moment. In this situation, the initial crystal field splitting is actually reduced. Correspondingly, the initial disproportionation in the occupation of the two orbitals is shrinking. We have verified that the *d*-only model shows the same kind of Hund's physics if we artificially consider the same *d*-electron occupation as in the *dp*-model.

Our findings have important consequences for LDA+DMFT calculations of transition metal oxides and related correlated materials: The physical results for *d*-only LDA+DMFT calculations can be dramatically different from calculations which also include the oxygen *p*-orbitals. Since the additional *p*-orbitals lead to a different *d*-filling the local interaction can result in the aforementioned dramatically different local DMFT physics. Eventually, experiments (such as, e.g., ARPES or X-ray absorption spectroscopy or orbital reflectometry) will show which of the two physical scenarios is correct.

Furthermore, as the *dp*-calculation is generally far away from an integer filling of the interacting *d*-orbitals, the observation of Mott-Hubbard metal-insulator transitions becomes more difficult[30, 31]. While one can expect non-local correlations beyond DMFT to be of importance for two-dimensional Mott insulators, not showing a Mott insulating phase in specific other cases might be a deficit of the *dp*-calculations – or, at least, of the way such *dp*-calculations are performed nowadays.

Let us emphasize that in other situations the physics of the *d*- and *dp*-calculation can be much more similar. This was e.g. observed for iron pnictides. In these materials, we have a large number of *d* electrons for both *dp*- and *d*-only calculation so that in both cases the physics is dominated by Hund's rule forming a local magnetic moment.

Acknowledgments

We acknowledge financial support from by the Deutsche Forschungsgemeinschaft (DFG) and the Austrian Science Fund (FWF) through the Research Units FOR 1346 (FWF I597-N16, A. T.) and FOR 1162 (DFG, N. P. and G. S.) and SFB ViCom F41 (K. H.). We thank S. Biermann M. Capone, A. Georges, M. Haverkort, J. Kuneš, L. de Medici, and P. Wissgott for fruitful discussions.

[1] J. Hubbard, Proc. Roy. Soc. London A **276**, 238 (1963); M. C. Gutzwiller, Phys. Rev. Lett. **10**, 159 (1963); J. Kanamori, Progr. Theor. Phy. **30**, 275 (1963).

[2] W. Metzner and D. Vollhardt, Phys. Rev. Lett. **62**, 324 (1989).

[3] A. Georges, G. Kotliar, W. Krauth, and M. Rozenberg, Rev. Mod. Phys. **68**, 13 (1996).

[4] V. I. Anisimov, A. I. Poteryaev, M. A. Korotin, A. O. Anokhin and G. Kotliar, J. Phys. Cond. Matter **9** (1997), 7359; A. I. Lichtenstein, and M. I. Katsnelson, Phys. Rev. B **57**, 6884 (1998); G. Kotliar, S. Y. Savrasov, K. Haule, V. S. Oudovenko, O. Parcollet and C. A. Marianetti, Rev. Mod. Phys. **78**, 865 (2006); K. Held, Adv. Phys. **56**, 829 (2007).

[5] N. F. Mott, Rev. Mod. Phys. **40**, 677 (1968); *Metal-Insulator Transitions* (Taylor & Francis, London, 1990); F. Gebhard, *The Mott Metal-Insulator Transition* (Springer, Berlin, 1997).

[6] K. Held, G. Keller, V. Eyert, D. Vollhardt, and V. I. Anisimov, Phys. Rev. Lett. **86** 5345 (2001).

[7] S. Y. Savrasov, G. Kotliar and E. Abrahams, Nature **410** 793 (2001).

[8] A. I. Lichtenstein, M. I. Katsnelson and G. Kotliar, Phys. Rev. Lett. **87** 067205 (2001).

[9] K. Held, A. K. McMahan and R. T. Scalettar, Phys. Rev. Lett. **87** 276404 (2001).

[10] M. Capone, M. Fabrizio, C. Castellani, and E. Tosatti, Science **296**, 2364 (2002).

[11] K. Byczuk, M. Kollar, K. Held, Y.-F. Yang, I. A. Nekrasov, T. Pruschke, and D. Vollhardt, Nature Physics **3**, 168 (2007).

[12] A. Toschi, M. Capone, C. Castellani, and K. Held, Phys. Rev. Lett. **102**, 076402 (2009).

[13] K. Haule, J. H. Shim, and G. Kotliar, Phys. Rev. Lett. **100**, 226402 (2008); L. Craco, M. S. Laad, S. Leoni, and H. Rosner, Phys. Rev. B **78**, 134511 (2008); K. Haule and G. Kotliar, New J. Phys. **11**, 025021 (2009); P. Hansmann, R. Arita, A. Toschi, S. Sakai, G. Sangiovanni, and K. Held, Phys. Rev. Lett. **104**, 197002 (2010); A. Toschi, R. Arita, P. Hansmann, G. Sangiovanni, K. Held, Phys. Rev. B **86**, 064411 (2012); N. Lanatá, H. U. R. Strand, G. Giovannetti, B. Hellsing, L. de' Medici, M. Capone, Phys. Rev. B **87** 045122 (2013)

[14] A. Valli, G. Sangiovanni, O. Gunnarsson, A. Toschi, and K. Held, Phys. Rev. Lett. **104**, 246402 (2010).

[15] M. Potthoff and W. Nolting, Phys. Rev. B, **60** 7834 (1999).

[16] S. Okamoto, Phys. Rev. Lett. **101**, 116807 (2008).

[17] P. Hansmann, Xiaoping Yang, A. Toschi, G. Khaliullin, O.K. Andersen, and K. Held, Phys. Rev. Lett. **103** 016401 (2009).

[18] P. Hansmann, A. Toschi, Xiaoping Yang, O.K. Andersen, K. Held, Phys. Rev. B, **82** 235123 (2010).

[19] M. Uchida, K. Ishizaka, P. Hansmann, Y. Kaneko, Y. Ishida, X. Yang, R. Kumai, A. Toschi, Y. Onose, R. Arita, K. Held, O. K. Andersen, S. Shin, and Y. Tokura, Phys. Rev. Lett. **106**, 027001 (2011); M. Uchida, K. Ishizaka, P. Hansmann, X. Yang, M. Sakano, J. Miyawaki, R. Arita, Y. Kaneko, Y. Takata, M. Oura, A. Toschi, K. Held, A. Chainani, O. K. Andersen, S. Shin, and Y. Tokura, Phys. Rev. B **84**, 241109 (2011).

[20] J. Chaloupka and G. Khaliullin, Phys. Rev. Lett. **100**, 016404 (2008).

[21] P. Hansmann, PhD Thesis, Vienna Unversity of Technology, Austria (April 2010).

[22] G. Wannier, Dynamics of Band Electrons in Electric and Magnetic Fields, Rev. Mod. Phys., **34**, 645 (1962); N. Marzari and D. Vanderbilt, Phys. Rev. B, **56**, 12847 (1997).

[23] O. K. Andersen, Electronic Structure and Physical Properties of Solids: The Uses of the LMTO method, Lecture Notes in Physics Springer, New York (2000).

[24] J. Kuneš, V. I. Anisimov, S. L. Skornyakov, A. V. Lukoyanov, and D. Vollhardt, Phys. Rev. Lett. **99**, 156404 (2007).

[25] J. Kuneš, L. Baldassarre, B. Schächner, K. Rabia, C. A. Kuntscher, Dm. M. Korotin, V. I. Anisimov, J. A. McLeod, E. Z. Kurmaev, and A. Moewes, Phys. Rev. B **81**, 035122 (2010).

[26] A. Perucchi, C. Marini, M. Valentini, P. Postorino, R. Sopracase, P. Dore, P. Hansmann, O. Jepsen, G. Sangiovanni, A. Toschi, K. Held, D. Topwal, D. D. Sarma, and S. Lupi, Phys. Rev. B **80**, 073101 (2009).

[27] J. Kuneš, V. Kŕápek, N. Parragh, G. Sangiovanni, A. Toschi, and A. V. Kozhevnikov, Phys. Rev. Lett. **109**, 117206 (2012).

[28] V. Kŕápek, P. Noák, J. Kuneš, D. Novoselov, Dm. M. Korotin and V. I. Anisimov , Phys. Rev. B **86**, 195104 (2012).

[29] M. Aichhorn, L. Pourovskii, V. Vildosola, M. Ferrero, O. Parcollet, T. Miyake, A. Georges, and S. Biermann, Phys. Rev. B **80**, 085101 (2009); S. L. Skornyakov, A. V. Efremov, N. A. Skorikov, M. A. Korotin, Yu. A. Izyumov, V. I. Anisimov, A. V. Kozhevnikov, and D. Vollhardt, Phys. Rev. B **80**, 092501 (2009); S. L. Skornyakov, A. A. Katanin, and V. I. Anisimov, Phys. Rev. Lett. **106**, 047007 (2011); M. Aichhorn, L. Pourovskii, and A. Georges, Phys. Rev. B **84**, 054529 (2011).

[30] K. Held, http://online.kitp.ucsb.edu/online/cem02/held (unpublished).

[31] Xin Wang, M. J. Han, Luca de' Medici, Hyowon Park, C. A. Marianetti, and Andrew J. Millis, Phys. Rev. B **86**, 195136 (2012).

[32] M.J. Han, Xin Wang, C.A. Marianetti, and A.J. Millis, Phys. Rev. Lett. **107** 206804 (2011).

[33] F. Lechermann, S. Biermann, and A. Georges, Progress of Theoretical Physics Supplement **160**, 233 (2005).

[34] Note: the completely filled t_{2g} orbitals can affect the broadening of the corresponding high-frequency part of the photoemission spectra, but *not* the low-energy electronic structures close to the Fermi level [35].

[35] X. Deng, M. Ferrero, J. Mravlje, M. Aichhorn, and A. Georges, Phys. Rev. B **85**, 125137 (2012).

[36] J. C. Slater and G. F. Koster, Phys. Rev. **94** 1498 (1954).

[37] V. I. Anisimov, J. Zaanen and O. K. Andersen, Phys. Rev. B **44** 943 (1991).

[38] M. Karolak, G. Ulm, T. O. Wehling, V. Mazurenko, A. Poteryaev, A. I. Lichtenstein, J. of Electron Spectroscopy and Related Phenomena, **181**,11 (2010).

[39] P. Werner and A. J. Millis, Phys. Rev. B, **74** 155107 (2006).

[40] E. Gull, A. J. Millis, A. I. Lichtenstein, A. N. Rubtsov, M. Troyer, P. Werner, Rev. Mod. Phys. **83**, 2 (2011)

[41] K. Haule, Phys. Rev. B **75**, 155113 (2007).

[42] N.Parragh, A. Toschi, K. Held, G. Sangiovanni, Phys. Rev. B, **86** 155158 (2012).

[43] E. Benckiser, M. Haverkort, *et al.* Nat. Materials (2011).

[44] Note that the sign of the Hartree difference depends also on the value of the Hund's exchange J (see also Ref. [33]). However, for plausible values of J, the condition $U > 5J$ is typically fulfilled, and, hence, the sign prefactor in Eq. 9 can be usually assumed as positive.

[45] Note that the trends emerging from our analysis have been tested to be quite stable against the changes of U, in a relatively broad range, while they are more sensible to changes of the Hund's exchange J, as will become clear from the discussion below.

[46] We note that the important physics driven by the Hund's exchange processes has attracted a considerable interest in the most recent literature[47–49].

[47] P. Werner, E. Gull, M. Troyer, and A. J. Millis, Phys. Rev. Lett. **101**, 166405 (2008).

[48] A. Georges, L. de' Medici, J. Mravlje, arXiv:1207.3033.

[49] L. de' Medici, Phys. Rev. B **83**, 205112 (2011) L. de' Medici, J. Mravlje, A. Georges, Phys. Rev. Lett. **107**, 256401 (2011).

[50] For example from constrained cRPA or even for cRPA locally unscreened calculations [51].

[51] Y. Nomura, M. Kaltak, K. Nakamura, C. Taranto, S. Sakai, A. Toschi, R. Arita, K. Held, G. Kresse, and M. Imada, Phys. Rev. B **86**, 085117, (2012).